A pathway linking translation stress to checkpoint kinase 2 signaling in *Neurospora crassa*

Axel C. R. Diernfellner[a,1], Linda Lauinger[a,2], Anton Shostak[a], and Michael Brunner[a,1]

[a]Biochemistry Center, Heidelberg University, D-69120 Heidelberg, Germany

Edited by Jay C. Dunlap, Geisel School of Medicine at Dartmouth, Hanover, NH, and approved July 18, 2019 (received for review September 7, 2018)

Checkpoint kinase 2 (CHK-2) is a key component of the DNA damage response (DDR). CHK-2 is activated by the PIP3-kinase-like kinases (PI3KKs) ataxia telangiectasia mutated (ATM) and ataxia telangiectasia and Rad3-related protein (ATR), and in metazoan also by DNA-dependent protein kinase catalytic subunit (DNA-PKcs). These DNA damage-dependent activation pathways are conserved and additional activation pathways of CHK-2 are not known. Here we show that PERIOD-4 (PRD-4), the CHK-2 ortholog of *Neurospora crassa*, is part of a signaling pathway that is activated when protein translation is compromised. Translation stress induces phosphorylation of PRD-4 by a PI3KK distinct from ATM and ATR. Our data indicate that the activating PI3KK is mechanistic target of rapamycin (mTOR). We provide evidence that translation stress is sensed by unbalancing the expression levels of an unstable protein phosphatase that antagonizes phosphorylation of PRD-4 by mTOR complex 1 (TORC1). Hence, *Neurospora* mTOR and PRD-4 appear to coordinate metabolic state and cell cycle progression.

checkpoint kinase 2 | translation inhibition | mTOR | *Neurospora crassa* | circadian clock

Checkpoint kinases 1 and 2 (CHK-1 and -2) play an important role in the DNA damage response (DDR). In mammals, DNA damage, e.g., by ionizing radiation or radiomimetic drugs, activates the PI3 kinase-like kinases (PI3KKs), ataxia telangiectasia mutated (ATM) and ataxia telangiectasia and Rad3-related protein (ATR), which phosphorylate and activate CHK-1 and CHK-2 (1). In higher eukaryotes, the PI3KK family member DNA-dependent protein kinase catalytic subunit (DNA-PKcs) can also activate CHKs (2–4).

Activated CHKs phosphorylate several targets, including phosphatases of the CDC25 family. This triggers proteasomal degradation of CDC25 and inhibits cell cycle progression by attenuating CDC25-dependent dephosphorylation and activation of cyclin-dependent kinases (CDKs). CHKs also phosphorylate (transcription) factors (e.g., p53) that activate the DNA repair machinery and induce apoptosis (1).

The activation pathway of CHK-2 is highly conserved. Initially, ATM and ATR phosphorylate CHK-2 at SQ/TQ sites (T68 by ATM in mammals) (5) in the SQ/TQ cluster domain (SCD) in the N-terminal portion of CHK-2. The phosphorylated SQ/TQ sites are recognized by the forkhead-associated (FHA) domain(s) of CHK-2, leading to transient homodimerization and subsequent autophosphorylation of CHK-2 at the activation loop of its kinase domain (6–8).

The circadian clock-controlled gene *prd-4* of the filamentous fungus *Neurospora crassa* was shown to encode a CHK-2 ortholog (9) involved in DNA damage response (10). In addition, activated PRD-4 induces hyperphosphorylation of the core circadian clock protein FREQUENCY (FRQ) and thereby advances the phase of the circadian clock (9). In mammals activated CHK-2 phosphorylates the core clock component PER1, triggering its degradation and advancing the phase of the circadian clock (11, 12). These observations suggested a DNA damage-induced signaling pathway to the circadian clock.

Treatment of *Neurospora* with the translation inhibitor cycloheximide (CHX) also triggers rapid hyperphosphorylation of FRQ (13) and pulse treatments with CHX cause phase advances of the clock (14, 15).

Here we identified PRD-4 as the kinase that phosphorylates FRQ in response to translation inhibition. The signaling pathway requires phosphorylation of SQ motifs by an upstream activating kinase distinct from the canonical upstream kinases ATM or ATR of the DDR. Our data suggest that the activating kinase is mechanistic target of rapamycin (mTOR), the central kinase of the TOR pathway. The TOR pathway is conserved in eukaryotes and regulates cellular growth and protein translation in response to nutritional status and stress (16). We show that translation stress is sensed via proteasomal degradation of an unstable inhibitor, presumably a phosphatase, which antagonizes phosphorylation of PRD-4 by mTOR.

Results

CHX-Induced Phosphorylation of FRQ Is Mediated by Activated PRD-4. Progressive phosphorylation of the *Neurospora* clock protein FRQ is dependent on CK1a (17), which interacts with FRQ-CK1a-interaction domain 1 (FCD1) and FCD2 in FRQ (13, 18). Treatment of *Neurospora* with the protein translation inhibitor CHX accelerated hyperphosphorylation of FRQ, suggesting a signal transduction from protein synthesis to the circadian clock of *Neurospora*. CHX-induced hyperphosphorylation was independent of FCD1 indicating that the reaction was not catalyzed by recruitment of CK1a (*SI Appendix*, Fig. S1*A* and ref. 13). To identify the signaling kinase, we screened a library (obtained from the Fungal Genetics Stock Center [FGSC]) of 51 homokaryotic kinase gene knockouts (*SI Appendix*, Table S1). CHX-induced

Significance

Checkpoint kinase 2 (CHK-2) is a key component of the DNA damage response (DDR) pathway and its activation mechanism is evolutionarily conserved. We show that PERIOD-4 (PRD-4), the CHK-2 ortholog of *Neurospora crassa*, is part of an additional signaling pathway that is activated when protein translation is compromised. Translation stress induces phosphorylation of PRD-4 by an upstream kinase distinct from those of the DDR pathway. We present evidence that the activating kinase is mTOR. Translation stress is sensed via a decrease in levels of an unstable inhibitor that antagonizes phosphorylation of PRD-4.

Author contributions: A.C.R.D. and M.B. designed research; A.C.R.D., L.L., and A.S. performed research; A.C.R.D. contributed new reagents/analytic tools; A.C.R.D. analyzed data; and A.C.R.D. and M.B. wrote the paper.

The authors declare no conflict of interest.

This article is a PNAS Direct Submission.

[1]To whom correspondence may be addressed. Email: axel.diernfellner@bzh.uni-heidelberg.de or michael.brunner@bzh.uni-heidelberg.de.

[2]Present address: Department of Biological Chemistry, School of Medicine, University of California, Irvine, CA 92697-1700.

This article contains supporting information online at www.pnas.org/lookup/suppl/doi:10.1073/pnas.1815396116/-/DCSupplemental.

Published online August 14, 2019.

hyperphosphorylation of FRQ was specifically compromised in the *Δprd-4* strain, which encodes an ortholog of CHK-2. When mycelial cultures of wild-type (*WT*) and *Δprd-4* strains were treated with CHX, the heterogeneously phosphorylated FRQ that accumulated in steady state in untreated light-grown mycelia was rapidly hyperphosphorylated in *WT* but not in *Δprd-4* (Fig. 1*A* and *SI Appendix*, Fig. S1*B*), indicating the requirement of PRD-4 in CHX-induced hyperphosphorylation of FRQ. We then tested the requirement of PRD-4 in vitro. Cell lysates were prepared from *WT* and *Δprd-4* mycelia that were previously treated with and without CHX. The lysates were then incubated with recombinant FRQ in the presence of ATP and phosphatase inhibitors (Fig. 1*B* and *SI Appendix*, Fig. S1 *C* and *D*). Cell lysate from CHX-treated *WT* supported hyperphosphorylation of recombinant FRQ, while lysate from CHX-treated *Δprd-4* mycelia or lysates from untreated mycelia did not. The data indicate that PRD-4 was activated in vivo upon inhibition of translation and subsequently phosphorylated recombinant FRQ in vitro.

Activation of PRD-4 by CHX Does Not Require the DDR Kinases ATM and ATR. PRD-4 was previously reported to hyperphosphorylate FRQ when activated by the radiomimetic drug methyl methanesulfonate (MMS) (9). MMS is an alkylating reagent that causes replication fork stalling and subsequent DNA double strand breaks. These activate the upstream kinases ATM and ATR, which then phosphorylate and activate CHK-2. Histone H2AX is also a substrate of ATM and ATR. Phosphorylated H2AX (γH2AX) accumulates at DNA double strand breaks and is widely used as an indicator of DNA damage and activation of ATM and ATR (19). We tested whether *Neurospora* ATM and ATR, encoded by *mus-21* and *mus-9*, respectively, phosphorylate H2AX in response to treatment with CHX (Fig. 2*A* and *SI Appendix*, Fig. S2*A*) or MMS (Fig. 2*B*). In *WT* cells, low levels of γH2AX were detected. The γH2AX level increased upon MMS treatment, but not upon treatment with CHX, which is not genotoxic. In contrast, only very little γH2AX was detected in a *mus-9^{ts}/Δmus-21* double mutant strain (gift from S. Tanaka, Saitama University, Saitama, Japan) (20), and γH2AX did not accumulate in this strain upon MMS treatment (Fig. 2*B*). The data indicate that *mus-21* and *mus-9* encode functional orthologs of ATM and ATR. Analysis of single mutants revealed that either kinase was able to phosphorylate H2AX (*SI Appendix*, Fig. S2*A*).

FRQ was efficiently hyperphosphorylated when *mus-9^{ts}/Δmus-21* mycelia were treated with CHX (Fig. 2*C* and *SI Appendix*, Fig. S2*B*). Hence, CHX-dependent activation of PRD-4 does not require the canonical upstream kinases of the DDR pathway. It should be pointed out that none of the 50 kinase *ko* strains that were tested in addition to *Δprd-4* showed a defect in activation of PRD-4 by CHX and subsequent phosphorylation of FRQ, indicating that the activating kinase was not covered by the *ko*-strain collection. To

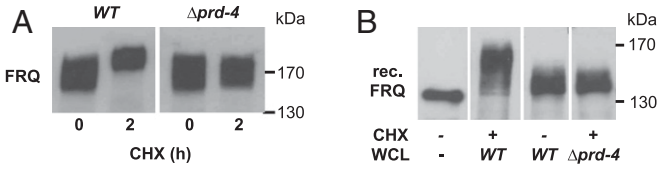

Fig. 1. *Neurospora* PRD-4 mediates CHX-induced hyperphosphorylation of FRQ. (*A*) CHX-dependent hyperphosphorylation of FRQ is impaired in a *prd-4* knockout strain. Liquid cultures of *WT* and *Δprd-4* strains were grown in constant light. Mycelia were harvested before and 2 h after addition of CHX. Western blots were decorated with antibodies against FRQ. (*B*) PRD-4 is active in extracts from cells pretreated with CHX. Purified recombinant FRQ (rec. FRQ) was incubated in the presence of ATP for 8 h at 22 °C with whole cell lysates (WCL) of *WT* and *Δprd-4* strains that were pretreated with or without CHX prior to harvesting. Western blots were decorated with FRQ antibodies.

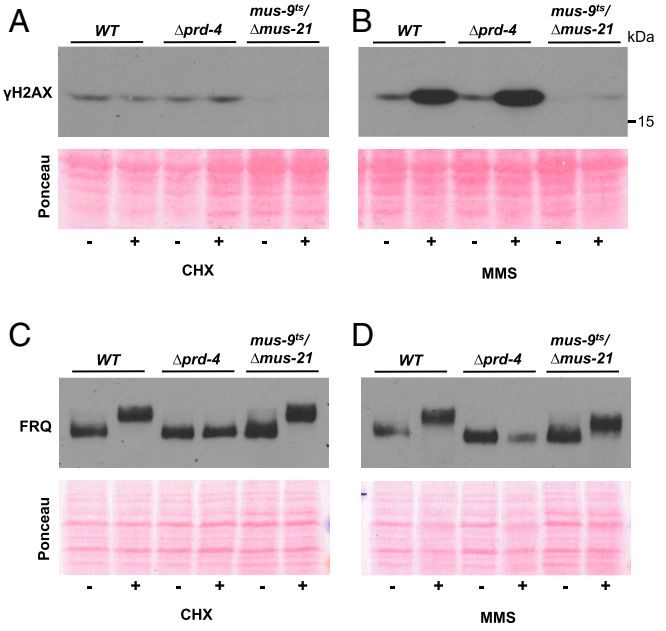

Fig. 2. CHX-induced activation of PRD-4 is independent of the upstream DDR kinases ATM (MUS-21) and ATR (MUS-9). Dark-grown mycelial cultures (10 h) of *WT*, *Δprd-4*, and *mus-9^{ts}/Δmus-21* (a mutant strain with a temperature-sensitive *mus-9* allele in a *Δmus-21* background) were exposed to a 2-h light pulse to induce synthesis of a wave of hypophosphorylated FRQ. Unless stated otherwise, all in vivo experiments presented in this work were conducted with hypophosphorylated FRQ produced under these culture conditions (corresponding to t = 0; see also *Materials and Methods*). The cultures were then incubated in the dark for another 2 h with or without CHX (*A* and *C*) or MMS (*B* and *D*). Western blots were then probed with antibodies against S129-phosphorylated histone H2AX (γH2AX) (*A* and *B*) or FRQ (*C* and *D*). Ponceau S stained membranes are shown for loading control.

our surprise, MMS triggered rapid hyperphosphorylation of FRQ in the *mus-9^{ts}/Δmus-21* strain (Fig. 2*D* and *SI Appendix*, Fig. S2*C*), indicating that MMS can activate PRD-4 by a pathway independent of the canonical DDR pathway.

Translation Inhibition Triggers PRD-4 Phosphorylation and Activation. To directly investigate the activation of PRD-4 we expressed in a *Δprd-4* strain a C-terminally His_6-2xFLAG-tagged PRD-4 protein ($PRD\text{-}4_{HF}$). Under standard growth conditions $PRD\text{-}4_{HF}$ accumulated in 2 distinct species, which correspond to hypo- and hyperphosphorylated isoforms, as assessed by phosphatase treatment (Fig. 3*A*). Exposure of mycelia to CHX induced further phosphorylation of both species of $PRD\text{-}4_{HF}$ (Fig. 3*A*). To determine whether $PRD\text{-}4_{HF}$ is also activated by other translation inhibitors, mycelia were treated with blasticidin and hygromycin, respectively (Fig. 3*B* and *SI Appendix*, Fig. S3*A*). Both inhibitors induced hyperphosphorylation of $PRD\text{-}4_{HF}$ and also of FRQ, suggesting that PRD-4 is generally activated when translation is compromised.

Pregueiro et al. used the radiomimetic drug MMS to induce the DNA damage response pathway in *Neurospora*, which led to hyperphosphorylation of FRQ (9, 21). However, MMS alkylates not only DNA but also RNA and was shown to inhibit translation in sea urchin embryos (22). Indeed, treatment of *Neurospora* with MMS efficiently inhibited light-induced synthesis of VIVID (VVD) (Fig. 3*C*), indicating that it inhibits protein expression (on the level of transcription and/or translation) in *Neurospora*. Thus, MMS, in addition to its genotoxic effect, inhibits directly and/or indirectly translation and thereby activates PRD-4 via the same pathway as CHX.

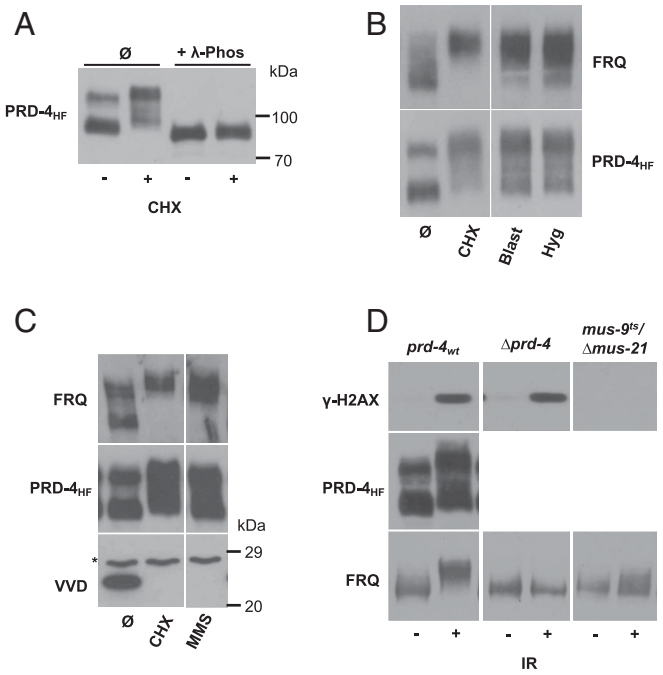

Fig. 3. Inhibition of translation triggers activation of PRD-4. (*A*) In vivo phosphorylation state of PRD-4_{HF}. A *Δprd-4* strain expressing C-terminally His_6-2xFLAG-tagged PRD-4 was created (*prd-*4_{wt}). Cultures of *prd-*4_{wt} were treated with and without CHX. WCLs were prepared and incubated with and without λ-phosphatase (1 h at 30 °C). The phosphorylation state of PRD-4_{HF} was analyzed by Western blot with FLAG antibodies. (*B*) Translation inhibition induces phosphorylation of PRD-4 and FRQ. Cultures were treated for 2 h with the protein translation inhibitors CHX, blasticidin (Blast), and hygromycin (Hyg), respectively. FRQ and PRD-4_{HF} were visualized on Western blots with FRQ and FLAG antibodies, respectively. (*C*) MMS is an inhibitor of protein expression. Dark-grown cultures (24 h) were exposed to a 2-h light pulse. When indicated, MMS or CHX was added to the growth medium 30 min prior to the light exposure. Samples were analyzed with FRQ and FLAG antibodies, and with antibodies against VVD, which is rapidly expressed in light. * indicates an nonspecific cross-reaction. (*D*) IR activates PRD-4 via the DDR pathway and triggers hyperphosphorylation of FRQ. Cultures of the indicated strains were exposed to Cs-137 radiation (200 Gy) and then analyzed by Western blot with γH2AX, FLAG, FRQ, and antibodies.

In order to trigger PRD-4 activation exclusively via the DDR pathway and not additionally by translation inhibition, we exposed *Neurospora* to ionizing radiation (IR) (Fig. 3*D*). Exposure to IR led to an increase in γH2AX levels, indicating that significant DNA damage had occurred and ATM and ATR were activated. PRD-4_{HF} was phosphorylated and FRQ was hyperphosphorylated in a PRD-4–dependent manner. Hyperphosphorylation of FRQ in response to IR was impaired in the ATM/ATR double mutant (*mus-*9^{ts}*/Δmus-21)*. Together our data indicate that PRD-4 can be activated by DNA damage via ATM and ATR and, in addition, by translation inhibition via a pathway independent of ATM and ATR. Treatment of *HEK293T* cells with CHX did not induce phosphorylation of human CHK-2 (*SI Appendix*, Fig. S3*B*). Similarly, CHX did not induce phosphorylation of the *Saccharomyces cerevisiae* CHK-2 orthologs, Rad53 and Dun1 (*SI Appendix*, Fig. S3 *C* and *D*). These preliminary analyses suggest that this pathway may not be widely conserved.

Translation Inhibition Activates an Upstream Kinase of PRD-4. To assess whether CHX-induced activation of PRD-4 is triggered by autophosphorylation or by an upstream kinase, we generated strains expressing kinase-dead versions of PRD-4_{HF}. Specifically, we generated PRD-4_{HF} versions with K319R and D414A substitutions, which correspond to the previously reported kinase-dead substitutions K249R (6) and D347A (7) in human and mouse CHK-2, respectively. Strains expressing PRD-4(K319R)$_{HF}$ or PRD-4(D414A)$_{HF}$ did not support CHX-induced hyperphosphorylation of FRQ, indicating that the mutant PRD-4 versions were inactive (Fig. 4 *A*, *Upper*). However, PRD-4 (K319R)$_{HF}$ and PRD-4(D414A)$_{HF}$ were both phosphorylated in response to CHX (Fig. 4 *A*, *Lower*), demonstrating that inhibition of translation activated an unknown upstream kinase of PRD-4.

Determination of PRD-4 Phosphorylation Sites. Activation of human CHK-2 is initiated predominantly by ATM but also by ATR, which phosphorylate SQ and TQ motifs, mainly Thr68, in the so-called SCD of the unstructured N-terminal portion (*SI Appendix*, Fig. S4*A*) (23). The N-terminal portion is followed by a FHA domain, which mediates transient homodimerization of CHK-2 by interacting with the phosphorylated SCD (6) and thereby allows autophosphorylation of the activation loop of the serine-threonine kinase domain. The kinase domain is followed by an unstructured C terminus, which contains a nuclear localization signal (NLS). PRD-4 carries in comparison to human CHK-2 N- and C-terminal extensions of 59 and 76 residues, respectively, which are predicted to be disordered (*SI Appendix*, Fig. S4*B*).

To characterize the pathway of PRD-4 activation in response to translation inhibition, we determined by mass spectrometry (MS) phosphorylation sites in PRD-4_{HF} and in catalytically inactive PRD-4(D414A)$_{HF}$ from mycelia treated with and without CHX (*SI Appendix*, Fig. S4*C*). In total we identified 36 phosphorylation sites (Fig. 4*B* and *SI Appendix*, Table S2). Eight sites were CHX dependent and found in PRD-4_{HF} as well as in the kinase-dead PRD-4(D414A)$_{HF}$, indicating that these sites were phosphorylated by a CHX-activated upstream kinase (Fig. 4*B*, blue). Of these 8 sites, 1 was found in the unstructured N terminus (S64), 4 were SQ motifs in the conserved SCD, 1 site was in the activation loop of the kinase domain (S444), and 2 sites were in the unstructured C-terminal portion of PRD-4 (S565, T566). Seven phosphorylation sites were CHX dependent and found in PRD-4_{HF} but not in PRD-4(D414A)$_{HF}$, suggesting that these were autophosphorylation sites of activated PRD-4 (Fig. 4*B*, red). Three autophosphorylation sites were located in the activation loop of the kinase (T446-448) and 4 autophosphorylation sites were located in the unstructured C-terminal portion of PRD-4. Of the remaining 21 phosphorylation sites 20 sites were clustered in the N-terminal region (residues 1 through 197) upstream of the FHA domain and one site was identified in the C-terminal portion. The extreme N terminus containing 6 sites was not covered in all samples analyzed by mass spectrometry, and it is therefore unclear whether phosphorylation of these sites was CHX dependent. The remaining 15 sites were found in absence and presence of CHX in *WT* and the kinase-dead PRD-4(D414A)$_{HF}$ protein. Since we did not perform quantitative mass spectrometry we do not know whether there are changes in abundance/prevalence of phosphorylation at these sites in response to CHX.

Pathway of CHX-Dependent Activation of PRD-4. To assess the function of PRD-4 phosphorylation we generated N-terminal deletions. Deletion of the N-terminal portion up to the SCD (aa 3 to 77 [Δ3-77]) removed 16 phosphorylation sites and deletion of residues 1 through 165 up to the FHA domain removed 23 phosphorylation sites. PRD-4(Δ3-77)$_{HF}$ and PRD-4(ΔN165)$_{HF}$ accumulated as single hypophosphorylated species (Fig. 4*C* and *SI Appendix*, Fig. S4 *D* and *E*). The data suggest that *Neurospora* accumulates 2 major species of PRD-4 that differ in phosphorylation of the unstructured N terminus upstream of the SCD. PRD-4(Δ3-77)$_{HF}$ was hyperphosphorylated in response to CHX and supported hyperphosphorylation of FRQ, while PRD-4(ΔN165)$_{HF}$ was neither hyperphosphorylated in presence of CHX nor did it

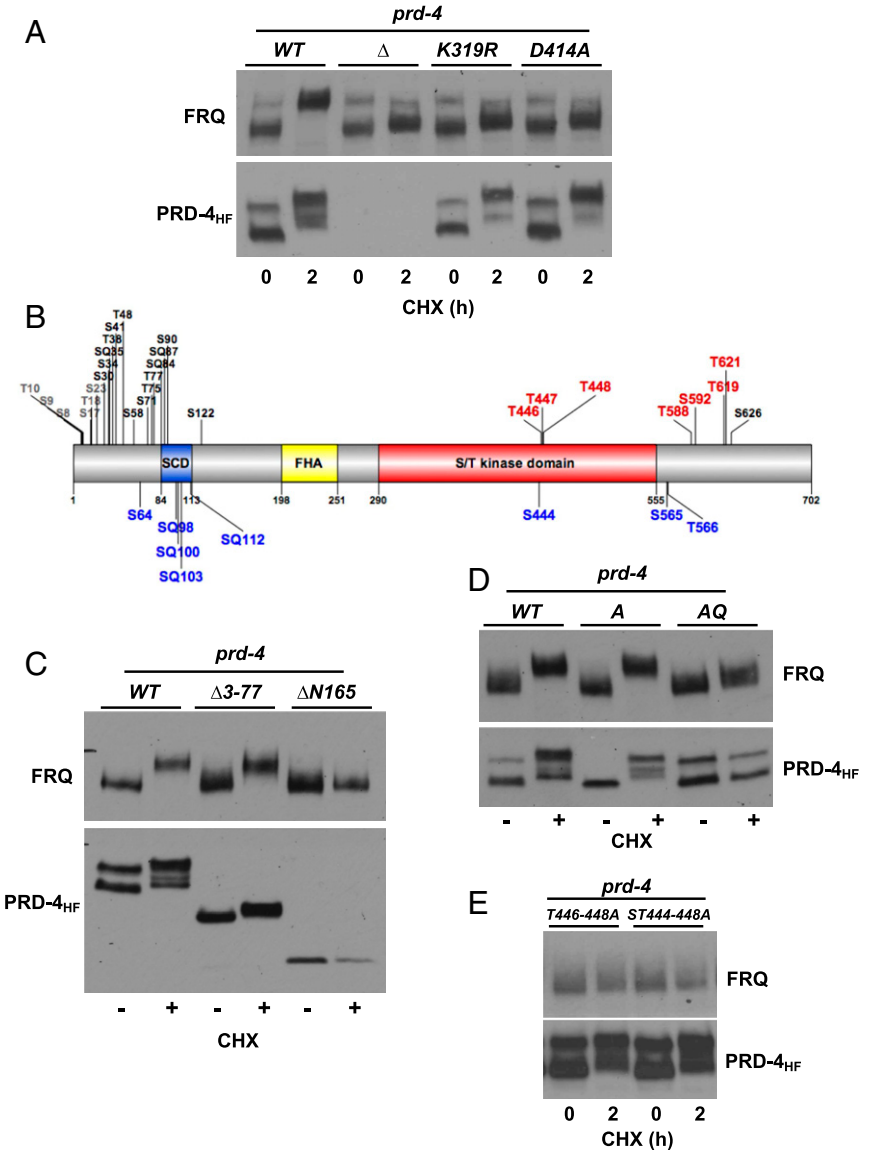

Fig. 4. Translation inhibition triggers phosphorylation of PRD-4 by an upstream kinase. (*A*) CHX induces phosphorylation of a kinase-dead version of PRD-4. Mycelial cultures of *Δprd-4* and of strains expressing tagged *WT* and kinase-dead versions of PRD-4 (*prd-4*$_{K319R}$ and *prd-4*$_{D414A}$) were harvested before and 2 h after incubation with CHX. Western blots were probed with FRQ and FLAG antibodies. (*B*) Schematic of *Neurospora* PRD-4 depicting phosphorylation sites identified by mass spectrometry. CHX-independent phosphorylation sites are shown in black. CHX-dependent phosphorylation sites found in PRD-4$_{HF}$ but not in the kinase-dead PRD-4(D414A)$_{HF}$ are shown in red, while CHX-dependent phosphorylation sites found in both PRD-4$_{HF}$ and PRD-4(D414A)$_{HF}$ are shown in blue. Gray: not classified due to low sequence coverage in some samples (*SI Appendix*, Table S2). SCD, SQ/TQ cluster domain; FHA, forkhead-associated domain. (*C*) The SCD is required for CHX-induced activation of PRD-4. Cultures of *prd-4*$_{wt}$, *prd-4*$_{Δ3–77}$, and *prd-4*$_{ΔN165}$ (*SI Appendix*, Fig. S4*D*) were incubated for 2 h with and without CHX. Whole cell lysates were prepared and analyzed by Western blot with FRQ and FLAG antibodies. (*D*) CHX-induced activation of PRD-4 requires phosphorylation of SQ sites in the SCD. Cultures of *prd-4*$_{wt}$ and of *prd-4*$_{A}$ (alanyl substitution of non-SQ sites in N-term) and *prd-4*$_{AQ}$ (alanyl substitution of SQ sites in SCD, see *SI Appendix*, Fig. S4*D*) were treated with and without CHX. The phosphorylation states of FRQ and PRD-4$_{HF}$ versions were analyzed. (*E*) Alanyl substitutions of T446-448 and S444, T446-448 in the activation loop result in kinase-dead versions of PRD-4$_{HF}$. Strains expressing the indicated PRD-4$_{HF}$ versions were incubated for 2 h with or without CHX and then analyzed.

support hyperphosphorylation of FRQ. The data demonstrate that the SCD is essential for CHX-dependent activation of PRD-4.

We then constructed 2 mutant versions, PRD-4(AQ)$_{HF}$ and PRD-4(A)$_{HF}$. In PRD-4(AQ)$_{HF}$ the 7 phosphorylated SQ motifs upstream of the FHA domain were changed to AQ, while in PRD-4(A)$_{HF}$ all phosphorylated S and T residues in the N-terminal portion (residues 1 through 165) except the SQ motifs were replaced by alanyl residues (Fig. 4*D* and *SI Appendix*, Fig. S4 *D* and *F*). In nonstimulated mycelia PRD-4(AQ)$_{HF}$ accumulated in a hypo- and a hyperphosphorylated pool, while PRD-4(A)$_{HF}$ was present as a single, hypophosphorylated species. The data suggest that the 2 major phosphorylated species of PRD-4 differ by CHX-independent phosphorylation of the N-terminal domain. CHX-induced phosphorylation of PRD-4(AQ)$_{HF}$ was impaired and the mutant protein did not induce hyperphosphorylation of FRQ. In contrast, PRD-4(A)$_{HF}$ was hyperphosphorylated and supported hyperphosphorylation of FRQ. The data demonstrate that CHX-dependent activation of PRD-4 requires phosphorylation of N-terminal SQ motifs.

To functionally characterize phosphorylation of the activation loop of PRD-4, we constructed strains expressing kinases with alanyl substitutions of S444, T446-448, and S444+T446-448,

respectively (Fig. 4*E* and *SI Appendix*, Fig. S4*G*). The 3 mutant kinases accumulated, like PRD-4_{HF}, in hypo- and hyperphosphorylated species and were phosphorylated in response to CHX treatment, suggesting that the upstream activation pathway was not affected. When cells were treated with CHX, PRD-$4(S444A)_{HF}$ supported hyperphosphorylation of FRQ, demonstrating that the kinase was active (*SI Appendix*, Fig. S4*G*). In contrast, the kinases with T446-448A and S444+T446-448A substitutions did not support hyperphosphorylation of FRQ (Fig. 4*E*). The data demonstrate that autophosphorylation of the activation loop is essential for activation of PRD-4 by CHX.

Alanyl-substitutions of the CHX-inducible phosphorylation sites in the C-terminal domain (*SI Appendix*, Table S2) had no detectable effect on PRD-4 activity (*SI Appendix*, Fig. S4*H*).

Together the results indicate that activation of PRD-4 by CHX is dependent on phosphorylation of SQ motifs in the N-terminal domain of PRD-4 by an upstream kinase followed by autophosphorylation of the activation loop of the kinase domain. Hence, translation inhibition induces activation of PRD-4 via a similar pathway as activation of human CHK2 by ATM and ATR in the DDR pathway.

Inhibition of mTOR Negatively Affects PRD-4 Activation. ATM and ATR belong to the family of PI3 kinase like protein kinases (PI3KKs). *Neurospora* encodes 2 more members of this family (24), the catalytically inactive TRA1/STK-18 subunit of SAGA and mTOR, the kinase subunit of mTOR complexes 1 and 2 (TORC1 and TORC2). TORC1 is activated by CHX (25, 26) via an increase in free amino acid levels and in mammals additionally via degradation of the unstable mTORC1 repressor REDD1 (27). We therefore asked whether treatment of *Neurospora* with CHX activates TORC1. Active TORC1 phosphorylates S6 kinase, which then phosphorylates the small ribosomal subunit protein S6 (16, 28). Activated TORC1 also induces via a multistep process dephosphorylation and activation of the translation initiation factor eIF2α (29, 30). To assess the phosphorylation status of S6 we expressed a hybrid S6 protein with the C terminus of *Homo sapiens* S6 that is recognized by a commercially available phospho-specific antibody (Fig. 5*A*). When *Neurospora* was treated with CHX, the hybrid S6 protein was phosphorylated and eIF2α was dephosphorylated (Fig. 5*B*), indicating that TORC1 was activated when translation was inhibited by CHX. Dephosphorylation of eIF2α and hyperphosphorylation of FRQ and PRD-4_{HF} exhibited similar sensitivity to CHX (*SI Appendix*, Fig. S5*A*). Hence, ATM/ATR-independent activation of PRD-4 correlates with CHX-dependent activation of TORC1.

Torin 2 is a highly potent and selective mTOR kinase inhibitor exhibiting a >100-fold selectivity over its related PI3KK family members ATM and ATR (31, 32). Treatment of *Neurospora* with Torin 2 reduced CHX-dependent phosphorylation of S6, indicating that mTOR was significantly inhibited (Fig. 5*C*), while the related PI3KKs, ATM and ATR, were not inhibited under such conditions (Fig. 5*D* and *SI Appendix*, Fig. S5*B*). Torin 2 treatment reduced the phosphorylation levels of PRD-4 and FRQ (Fig. 5*C* and *SI Appendix*, Fig. S5*C*), suggesting that mTOR is the upstream PI3KK that activates CHK-2 in response to translation stress.

Role of Phosphatases in PRD-4 Activation. The activity of TORC1 is dependent on the metabolic state of the cell and TORC1 is active to various extents under a broad variety of physiological

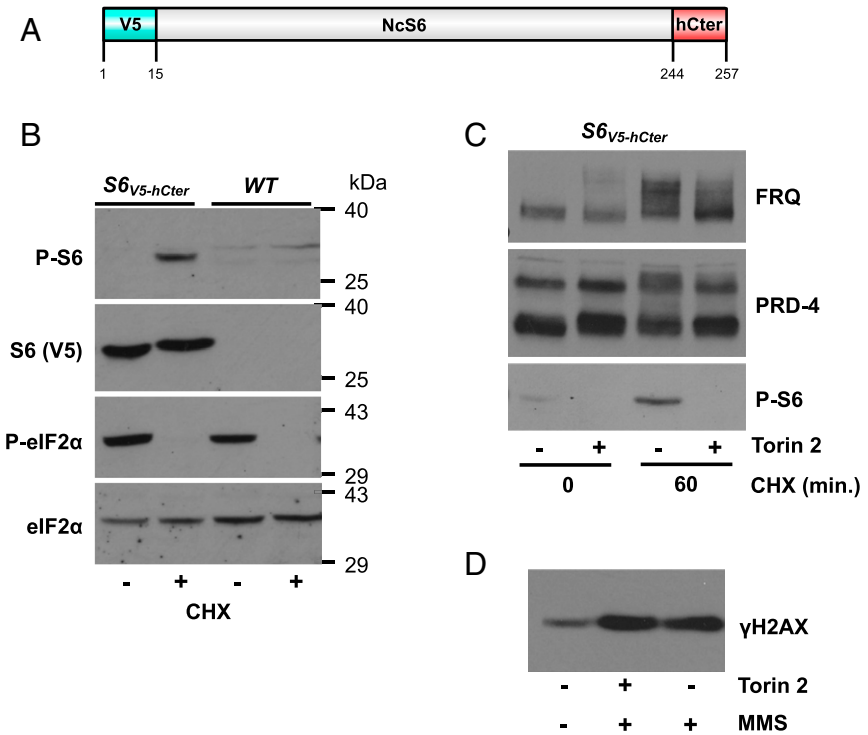

Fig. 5. CHX activates the TORC1 pathway. (*A*) Schematic of a chimeric *Neurospora* ribosomal S6 protein carrying the C terminus of human S6 to allow for detection with phospho-specific antibodies against human S6. The protein is additionally tagged with an N-terminal V5 epitope ($S6_{V5\text{-}hCter}$). (*B*) CHX induces phosphorylation of S6 and reduces phosphorylation of eIF2α. Cultures of $S6_{V5hCter}$ and *WT* were treated with and without CHX for 2 h prior to harvesting. Western blots were decorated with phospho-S6 and V5 antibodies as well as with antibodies against phospho-eIF2α and eIF2α. (*C*) Kinetics of PRD-4 and FRQ phosphorylation are impaired by inhibition of mTOR. Cultures of $S6_{V5\text{-}hCter}$ were treated for 5 h with and without 15 μM Torin 2. Subsequently, 0.1 μg/mL CHX was added and mycelia were harvested after the indicated time periods. Western blots were decorated with FRQ, PRD-4, and phospho-S6 antibodies. (*D*) Torin 2 does not inhibit the mTOR-related PI3KKs, ATM and ATR. Cultures of $S6_{V5\text{-}hCter}$ were either supplied with 15 μM Torin 2 for 5 h or left untreated before the addition of MMS. Mycelia was harvested 2 h after addition of MMS. Western blot was decorated with γH2AX antibodies (see also *SI Appendix*, Fig. S5*B*).

conditions. Since PRD-4 is not active under standard growth conditions, it seems plausible that TORC1-dependent activation of PRD-4 is normally inhibited and will be activated only under stress condition when protein translation is compromised. Conceptually, inhibition of protein translation (translation stress) could be sensed by the decrease of the steady-state level of an unstable inhibitor of the PRD-4 signaling pathway. To assess whether the CHX-induced activation of PRD-4 is dependent on protein turnover, we inhibited the ubiquitin proteasome system with thiolutin (THL), a potent inhibitor of the proteasomal deubiqitinase RPN11 (33). Treatment of mycelial cultures with THL together with CHX suppressed hyperphosphorylation of PRD-4_{HF} (Fig. 6 *A*, *Upper*). Furthermore, lysates prepared from such cells did not support hyperphosphorylation of recombinant FRQ (Fig. 6 *A*, *Lower*). These data demonstrate that inhibition of protein synthesis did not activate PRD-4 under conditions when protein degradation was also compromised. THL did not prevent activation of PRD-4 by MMS, indicating that the DDR pathway was not compromised when the proteasome was inhibited (*SI Appendix*, Fig. S6*A*). The data are compatible with the notion that phosphorylation and activation of PRD-4 is tightly suppressed by an unstable inhibitor, which is constitutively synthesized. When protein translation is compromised the previously synthesized inhibitor is rapidly degraded and thereby shifts the system toward phosphorylation and activation of PRD-4 by TORC1.

To address whether the unstable protein in question could be a phosphatase, mycelia expressing PRD-4_{HF} were incubated with and without phosphatase inhibitors (Fig. 6*B* and *SI Appendix*, Fig. S6*B*). Subsequently, the phosphorylation status of newly synthesized FRQ was analyzed, which is a highly sensitive indicator of PRD-4 activity. In the presence of phosphatase inhibitors the phosphorylation state of FRQ was elevated in a PRD-4 dependent manner, indicating that phosphatase inhibition activated PRD-4 even in the absence of translation stress.

Activation of PRD-4 by phosphatase inhibitors was independent of ATM and ATR but required the SQ motifs in the SCD (*SI Appendix*, Fig. S6 *C* and *D*), suggesting that phosphorylation of the SCD of PRD-4 by mTOR is antagonized by its dephosphorylation by an unstable phosphatase (or a phosphatase regulator).

Impact of Translation Inhibition on the Circadian Clock. Pulse treatment of *Neurospora* with CHX was shown to shift the phase of the circadian clock (14, 34). Similar results were obtained when *Neurospora* was pulse treated with MMS (9). The phase response to MMS was largely abolished in a *Δprd-4* background (9). To assess the potential role of PRD-4 in the CHX-dependent phase shift, we analyzed in *WT* and *Δprd-4* strains expression of the circadian luciferase reporter *frq-lucPEST* (35). Synchronized mycelial cultures of *WT* and *Δprd-4* were treated with 1-h pulses of CHX. Subsequently *frq-lucPEST* bioluminescence rhythms were recorded to determine the CHX-dependent phase shift of the circadian clock (Fig. 7*A* and *SI Appendix*, Fig. S7*A*). CHX treatment of *WT* induced mainly phase advances with the largest advance around subjective noon. These data are consistent with previous findings of Nakashima et al. (14). In stark contrast, CHX treatment of *Δprd-4* induced a large phase delay of about 6 h independently of the circadian time the drug was administered. A CHX pulse inhibits protein synthesis for a certain time period until cells recover, and thereby causes a delay of (all or most) biochemical reactions. Apparently, this general effect of CHX caused in the *Δprd-4* strain the phase delays of the circadian clock.

In *WT* cells CHX additionally activates PRD-4, which accelerates hyperphosphorylation of FRQ and thereby advances the phase of the circadian clock. The phase advance is small when CHX is given at times when FRQ was already hyperphosphorylated and large at times when FRQ was hypophosphorylated. Thus, the actually observed phase response in *WT* is the delta between the general CHX-dependent delay and the PRD-4 specific, time-of-day–dependent phase advance.

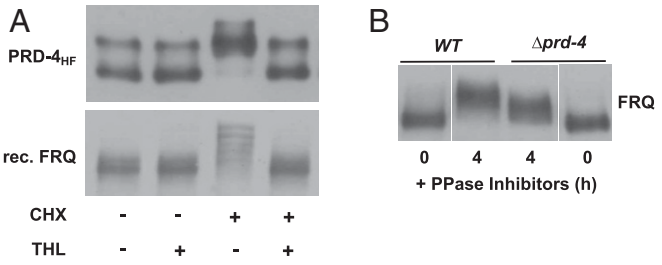

Fig. 6. Activation of PRD-4 by CHX is promoted by the proteasome and antagonized by phosphatase. (*A*) Inhibition of the proteasome with THL prevents activation of PRD-4 by CHX. Dark-grown cultures (40 h) were treated for 30 min with or without THL and then for 2 h with or without CHX, as indicated. Whole cell lysates were prepared and in vitro phosphorylation of recombinant FRQ was performed as described in Fig. 1*B*. Western blots were probed for PRD-4 and FRQ. (*B*) Inhibition of phosphatases promotes PRD-4–dependent hyperphosphorylation of FRQ in the absence of CHX. A mixture of phosphatase inhibitor was added to *prd-4*$_{wt}$ and *Δprd-4*. Cultures were harvested at time 0 and after 4 h, and the phosphorylation state of FRQ was analyzed.

Discussion

We describe a signal transduction pathway that activates the *Neurospora* checkpoint kinase 2 ortholog PRD-4 in response to inhibition of protein translation (Fig. 7*B* and *SI Appendix*, Fig. S7*B*). Activated PRD-4 phosphorylates the clock protein FRQ and thereby advances the phase of the circadian conidiation rhythm. We show that activation of CHK-2 by ionizing radiation also induces hyperphosphorylation of FRQ. The data suggest that both stress signals overwrite the clock-dependent conidiation process to accelerate the production of asexual spores, potentially as a survival strategy.

Initial characterization of this pathway revealed that activation of PRD-4 by translation stress is dependent on an upstream kinase. This kinase is distinct from the canonical upstream kinases, ATM and ATR, which activate PRD-4 in response to DNA damage. Yet, the activation pathway of PRD-4 by CHX corresponds to the conserved activation pathway of mammalian CHK-2 by ATM. Thus, activation of PRD-4 by translation inhibition requires phosphorylation of N-terminal SQ motifs followed by autophosphorylation of PRD-4 in the activation loop of its kinase domain. It seems therefore conceivable that the upstream activating kinases are related. ATM and ATR belong to the family of PI3KKs. DNA-PKcs, a PI3KK family member that can also activate CHK2, is not expressed in lower eukaryotes, including *Neurospora*. The only additional catalytically active PI3KK member in *Neurospora* is mTOR, the kinase subunit of TORC1 and TORC2. We show that *Neurospora* TORC1 was activated by inhibition of translation, and specific inhibition of mTOR with Torin 2 compromised the activation of PRD-4 by CHX. Hence, our data indicate that TORC1 is the upstream kinase complex that activates PRD-4 in response to inhibition of protein translation. A knockout of VTA, a TORC1-associated regulatory component, was shown to dampen the FRQ protein rhythm (36), suggesting a connection with the *Neurospora* circadian clock.

Although TORC1 activity is stimulated by CHX, it is already active under standard growth conditions in the absence of CHX. Hence, the TORC1-dependent activation of PRD-4 must be antagonized under normal (unstressed) conditions.

We show that inhibition of the proteasome with THL suppressed activation of PRD-4 by translation stress. We therefore hypothesize that the signal transduction pathway senses protein homeostasis, and ultimately translation stress, by assessing the

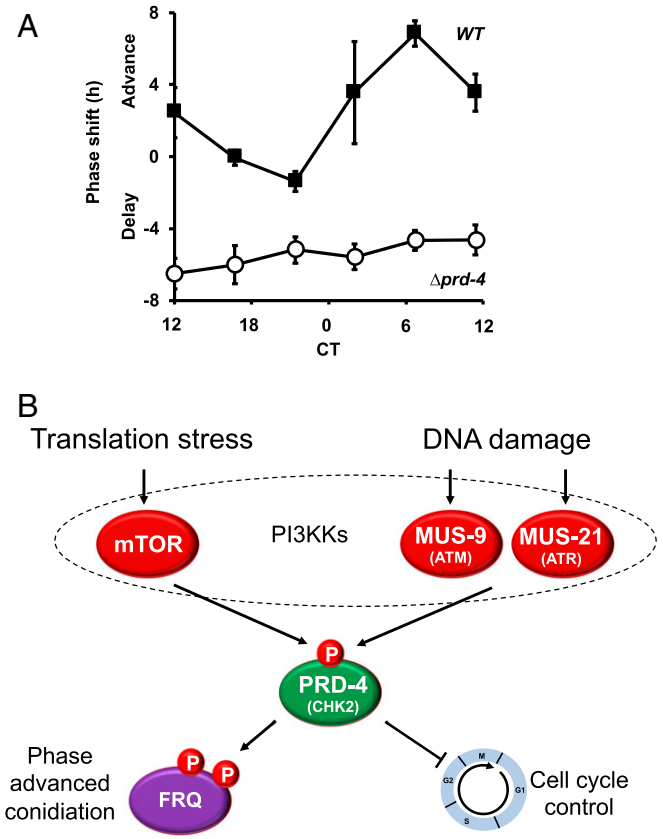

Fig. 7. CHX induces circadian phase shifts in a PRD-4–dependent manner. (*A*) CHX resets the circadian clock in a PRD-4 and clock-specific manner. Mycelial discs of *WT* and *Δprd-4* strains expressing *frq-lucPEST* were grown in liquid medium. The cultures were transferred to darkness in order to reset the clock to circadian time 12 (CT12). At the indicated circadian time, discs were treated for 1 h with or without CHX and then placed on solid growth medium supplied with luciferin. Circadian bioluminescence rhythms were then measured over the course of 3 d (*SI Appendix*, Fig. S7*A*). The phase shift of *frq-lucPEST* rhythms induced by CHX was blotted versus the circadian time. (CT12 corresponds to subjective dusk; CT0 to subjective dawn.) *WT*, black squares; *Δprd-4*, open circles. Error bars indicate ±SEM (n = 4). (*B*) Model of translation stress and DNA damage that activate *Neurospora* CHK2 (PRD-4) via distinct PI3KKs, mTOR and ATM/ATR, respectively. Activated PRD-4 promotes cell cycle arrest and advances the circadian phase of clock-controlled conidiation rhythm.

balanced steady-state levels of a constitutively expressed highly unstable antagonist of mTORC1.

Inhibition of protein synthesis in mammals leads to a rapid loss of the highly unstable mTORC1 inhibitor REDD1 and subsequently derepression of mTORC1. However, REDD1 and its targets TSC1 and TSC2 are not expressed in *Neurospora*.

Instead, the unstable inhibitor in *Neurospora* appears to be or regulate a phosphatase that antagonizes activation of PRD-4 by TORC1. In fact, inhibition of phosphatases activated PRD-4 (independently of ATM and ATR) even in the absence of CHX, which is compatible with the notion that the activating kinase is active under normal growth conditions. TORC1 supports translation according to the metabolic state of the cell. Since expression levels of the unstable inhibitor should also depend on TORC1 activity, the repressed (clamped) state of the pathway could easily adapt to different growth rates (TORC1 activity levels), and PRD-4 would only be activated by translation stress, i.e., when protein synthesis and degradation become unbalanced (*SI Appendix*, Fig. S7*B*).

In summary, we uncovered a pathway in *N. crassa* that transduces translation stress to checkpoint kinase 2 signaling, probably via TORC1. Although we have no evidence that the pathway is widely conserved, it provides a paradigm showing that a CHK-2 can in principle be activated by stress signals that are not associated with DNA damage.

Materials and Methods

***Neurospora* Strains and Culture Conditions.** *Neurospora* strains *Δprd-4* (FGSC 11169 and 11170), *mus-9* (*Δatr*, FGSC 15893), *mus-21* (*Δatm*, FGSC 11162), as well as the kinase knockout library were obtained from FGSC (Manhattan, KS). The above listed knockouts were created by the functional genomics program (37). The *mus-9^{ts}/mus-21* (*atr^{ts}/Δatm*) strain was a generous gift from S. Tanaka (20). *frqΔFCD1* (13) carried the ras-1^{bd} (38) mutation. All knockout strains carried the hygromycin resistance cassette. The *WT* strain used was 74-OR23-1VA.

For transformations, *Δprd-4, ras-1^{bd}, his-3, mat a* was used, which was created by crossing *Δprd-4, mat a* with *ras-1^{bd}, his-3, mat A* using standard crossing protocol (39). Conidial suspensions in 1 M sorbitol were prepared from strains grown (5 to 7 d) on standard solid growth medium (2.2% agar, 0.3% glucose, 0.17% L-arginine, 1× Vogel's medium, and 0.1% biotin). Standard growth medium for liquid cultures contained 2% glucose, 0.17% L-arginine, and 1× Vogel's medium.

To obtain a population of predominantly hypophosphorylated newly synthesized FRQ in order to better compare phosphorylation state and kinetics in the various strains, cultures were grown for 32 to 36 h in constant light at 25 °C prior to a transfer into darkness for 10 h. During this time, FRQ progressively hyperphosphorylates and almost completely degrades (13). An ensuing 2-h light pulse prior to another release into constant darkness leads to light-induced expression of a new population of hypophosphorylated FRQ, which—unless otherwise stated—corresponds to t = 0 of treatment with antibiotic, chemical agent, or irradiation. CHX was used at a concentration of 10 μg/mL unless stated otherwise. Blasticidin (50 μg/mL; Gibco), 50 μM thiolutin (Carbosynth), 1% MMS (Sigma-Aldrich), and 800 μg/mL hygromycin B (Sigma-Aldrich) final concentrations were used unless otherwise indicated in the text. mTOR inhibitor Torin 2 (LC Laboratories) was used at 15-μM final concentration. For in vivo phosphatase inhibition, cultures were treated as previously described (13). Western blots shown are representative results from experiments that were performed at least 3 times.

Plasmids and Constructs. A modified pBM61 his-3 targeting vector, pFH62, containing a trpC terminator sequence immediately following the multiple cloning site was used as the backbone for the cloning of *Neurospora* checkpoint kinase 2. A genomic fragment containing promoter (from −1350) and ORF of prd-4 was amplified using the primers prd-4 F *Spe*I (5′-TTTTTTTACTAGTGAAG AAGAGCTGTTCTGTG-3′) and prd-4 R his6 2xflag *Asc*I (5′-GGCGCGCCTTACTTATCGTCGTCA TCCTTGTAATCTTTGTCATCATCGTCTTTG-TAGTCGTGATGGTGGTGATGGTGTTTTTTCTTACCCTTACCCTTAC-3′). The fragment was cloned into pFH62 using *Spe*I and *Mlu*I to create pFH62 pprd-4::prd-4-His$_6$-2xFLAG (prd-4$_{wt}$). This plasmid was used as the source to create all prd-4 mutant versions used in this paper. The mutants prd-4$_{K319R}$ (corresponds to mammalian kinase-dead mutant K249R; F: 5′-[Phos]TATGCCGTCAGGGTGTTCTCC-3′, R: 5′-[Phos]CTGTGTACCCGTCGACTTC-3′), prd-4$_{D414A}$ (corresponds to mammalian kinase-dead mutant D347A; F: 5′-[Phos]GTCCACCG CGCCATCAAACCC-3′, R: 5′-[Phos]AATGTTGCGGTCGTGCAAG-3′), prd-4$_{S444A}$ (F: 5′-CGGCGAGGAAGCTTT-CACTACTAC-3′, R: 5′-GTAGTAG TGAAAGCTTCCTCGCCG-3′), prd-4$_{ST565-566A}$ (F: 5′-CCTGGCGTCAA CGACGCCGCCAACGGCCTTG-3′, R: 5′-CAAGGCCGTTGGCGGCGTCGTT GACGCCAGG-3′), prd-4$_{ST444-448A}$ (F: 5′-GATCATCGGCGAGGAAGC CTTCGCGGCCGC-TCTCTGTGGTACGCC-3′, R: 5′-GGCGTACCACAG AGAGCGGCCGCGAAGGCTTCCTCGC-CGATGATC-3′) and prd-4$_{T446-448A}$ (F: 5′-GATCATCGGCGAGGAATCCTTCGCGGCCG-CTCTCTGTGGTACGCC-3′, R: 5′-GGCGTACCACAGAGAGCGGCCGCGAAGGATTCCTCGCCGA TGATC-3′) were created via site-directed mutagenesis using standard protocols. prd-4$_{ΔN165}$ (deletion of aa 2 through 165) was created by deletion mutagenesis (F: 5′-TTTGGCGCGCCATGGCGGTTGGCTCCAAGAGAG-3′, R: 5′-TTTGGCG-CGCCGGCTGCTGGGATTGTAGGG-3′). prd-4$_{Δ3–77}$ was created by deletion mutagenesis (F: 5′-CCCAGCAGCCATGGCTCCTCC AGCC-3′, R: 5′-GGCTGGAGGAGC CATGGCTGCTGGG-3′). The N-terminal multiple phosphorylation site mutants prd-4$_{A}$ and prd-4$_{AQ}$ were created by gene synthesis (Genscript; see *SI Appendix* for sequences). Plasmid for expression of 2xFlag-tagged Dun1 in yeast (generous gift of Hurt group/Heidelberg University Biochemistry Centre, Heidelberg, Germany) was based on 4383-YCp111-P.ADH1-HA-RSA4. PCR product (F: 5′-TTTGGATCC AGTTTGTCCACGAAAAGAGAGC-3′, R: 5′-TTTGCGGCCGCT TAGAG GCAAGATAATTCTGAGTATG-3′) amplified from cDNA was inserted using *Bam*HI-*Not*I.

Ribosomal protein S6 was N-terminally V5-tagged and the C-terminal motif surrounding phosphosites S235/236 was modified to be identical to human S6 (in order to be able to use commercially available phospho-S6

[S235/236] antibody [Cell Signaling #2211]) to create $S6_{hCter}$. Accordingly, the C terminus was changed from DARKRRA**SS**MRK to EQIAKRRRL**SS**LRA via amplification of a genomic fragment with primers containing V5-tag and the modified 3′ region (F: 5′-TTTTTGAATTCACCATGGGTAAGCCTATCCCTA ACCCTCTCCTCGGTCTCGATTCTACGGGAGGTAAGGTACGACGACTCCCC-3′, R: 5′-TTTTTTTGCGGCCGCTTACGCGCGCAGGGAGGAGAGGCGGC GGCGCTTGGC GATCTGCTCGGCCTTCTGGACCTTG-3′). The fragment was cloned into pFH72 (a modified pBM61 his-3 targeting vector containing a ccg-1 promoter and a trpC terminator sequence immediately upstream and downstream of the multiple cloning site) using *Eco*RI-*Not*I.

Protein Extraction. For the extraction of *Neurospora* native protein, tissue/cells were ground in the presence of liquid nitrogen using a precooled pestle and mortar. The powder was suspended in extraction buffer (50 mM Hepes/KOH [pH 7.4], 137 mM NaCl, 10% [vol/vol] glycerol, 5 mM EDTA containing 1 mM PMSF, 5 μg/mL leupeptin, and 5 μg/mL pepstatin A) (see also ref. 40). Protein concentrations were determined by NanoDrop (PeqLab). Generally, 200 μg of *Neurospora* whole cell lysate was analyzed by SDS/PAGE and transferred to a nitrocellulose membrane (GE Healthcare; 0.45 μm, 10 × 150 cm). The membrane was blocked with TBS and 5% milk (pH 7.4) prior to incubation with antibodies (see also refs. 17 and 40). Antibodies α-γH2AX (α-H2A pS129, abcam, ab15083), α-eIF2α (abcam, ab47508), α-P-eIF2α (α-eIF2α pS51, abcam, ab32157), α-FLAG (Sigma-Aldrich) were used at the recommended dilutions and α-FRQ (17) at 1:20 in TBS with 5% milk.

To obtain PRD-4 antibodies cDNA from mRNA extracted from *prd-4*$_{wt}$ was used to amplify and clone the ORF of C-terminally His_6-2xFLAG-tagged PRD-4 into a pET expression vector. PRD-4_{HF} was then overexpressed in Rosetta (Novagen) cells and purified over a Ni-NTA column as per standard manufacturers' protocols. The purified recombinant protein was used to generate rabbit polyclonal PRD-4 antibody (Pineda, Germany). Rabbits were killed 91 d postimmunization and affinity purified PRD-4 antibody was used at a dilution of 1:500 in TBS with 5% milk.

Denatured yeast protein extracts were done as described (41). α-Rad53 (abcam, ab104232) was used as recommended.

In Vitro Phosphorylation. The phosphorylation reaction contained 50 mM Hepes/KOH, pH 7.4, 150 mM NaCl, 10 mM $MgCl_2$, 10 mM ATP, leupeptin (2 μg per mL), pepstatin A (2 μg per mL), PMSF (1 mM), and PhosStop phosphatase inhibitor mixture (Roche). A total of 100 ng of recombinant FRQ (41) was incubated with 400 μg of *Neurospora* whole cell lysate in a final volume of 60 μL at 22 °C for 8 h. A total of 20 μL 4× Laemmli sample buffer was added, followed by a 5-min incubation at 95 °C. Ten-microliter aliquots were analyzed by SDS gel electrophoresis followed by Western blot analysis with FRQ antibody.

Protein Dephosphorylation. In a total volume of 50 μL, 100 μg of whole cell lysate was incubated with 5 μL 10xPMP buffer (New England Biolabs), 5 μL $MnCl_2$, and 800 units λ-phosphatase (NEB) for 1 h at 30 °C.

γ-Irradiation. For γ-irradiation, liquid cultures were transferred to black light-tight 50 mL Falcon tubes and placed into a Gammacell1000D irradiation chamber (Best Theratronics, Canada) containing 4 Cs-137 sources (combined dose: 8.33 Gy/min). The irradiated cultures received a dose of 200 Gy, while controls were left outside of the chamber.

α-FLAG Immunoprecipitation of PRD-4 and Mass Spectrometry. Liquid cultures of *Neurospora* strains prd-4_{wt} and prd-4_{D414A} were incubated in constant light at 25 °C for 2 d and then either treated with CHX for 2 h or left untreated prior to harvesting. The frozen mycelia were ground to fine powder and cells were lysed by vortexing in TAP buffer (50 mM Tris–HCl, pH 7.5, 150 mM NaCl, 1.5 mM MgCl2, 0.1% Nonidet P-40, 0.5 mM DTT, 1 mM PMSF, 1 μg/mL Leupeptin, 1 μg/mL Pepstatin A, and PhosStop). A preclearing centrifugation step was done for 30 min at 10,000 rpm (JA-10 rotor). Supernatants were combined and ultracentrifuged (38,000 rpm 1 h, Sorvall WX ultracentrifuge, T647.5 rotor). Anti-FLAG beads (ANTI-FLAG M2 Affinity Gel, Sigma-Aldrich) were washed (3× in PBS) and blocked with 5% milk in PBS for 1 h at room temperature followed by another wash (3× in TAP buffer). Approximately 500 mg of the cleared protein extracts were incubated with 175 μL beads and rotated overnight at 4 °C. Beads were then transferred to 1.5-mL tubes and washed (3× with PBS supplied with protease inhibitors). Finally, beads were incubated with 150 μL of 2× LDS sample buffer (Invitrogen) supplied with 100 mM DTT at 72 °C for 15 min. A total of 2× 60 μL per sample was loaded on a 12% PAA gel, which was stained with Coomassie. All samples were digested with trypsin or elastase prior to MS. The mass spectrometry for identification of the phosphorylation sites was performed as described (42).

Phase Response Curve. Petri dishes containing liquid Vogel's media were inoculated with conidia from *Δprd-4, ras-1*^{bd}*, pfrq::lucPEST*; and *WT, ras-1*^{bd}*, pfrq::lucPEST* (both strains expressing destabilized luciferase under the control of the circadian clock-regulated *frq* promoter, respectively) (35) and incubated without shaking at 25 °C in constant light for 36 h. From the resulting mycelial mats, discs were punched out, distributed to Erlenmeyer flasks containing liquid medium (0.05% fructose, 0.05% glucose, 2% sorbose, 1× Vogel's, 10 ng/mL biotin) and further incubated in constant light at 25 °C shaking. In 4-h intervals, cultures were then transferred to darkness over a 20-h period. Half of the samples were then pulsed with 10 μg/mL CHX for 1 h, while the other half was left untreated. Discs were then rinsed and excess liquid was removed with sterile paper towels and placed on solid medium containing luciferin (35) in 24-well plates. Luminescence was recorded over a period of 72 h every 30 min in constant darkness using an EnSpire Plate reader (Perkin-Elmer).

ACKNOWLEDGMENTS. We thank Sabine Schultz for continuous excellent technical assistance and Barbara Kahn-Schapowal (DKFZ) and the DKFZ, Heidelberg for help and permission to use the irradiation chamber. We also thank Dr. Shuuitsu Tanaka (Saitama University, Japan) for providing the *mus-9*^{ts}*/mus-21* strain and the Fungal Genetics Stock Center (Manhattan, KS) for providing the other knockout strains. This work was supported by the Deutsche Forschungsgemeinschaft DI 1874/1-1 (to A.D.) and SFB1036 (to M.B.).

1. T. H. Stracker, T. Usui, J. H. Petrini, Taking the time to make important decisions: The checkpoint effector kinases Chk1 and Chk2 and the DNA damage response. *DNA Repair (Amst.)* **8**, 1047–1054 (2009).
2. J. Li, D. F. Stern, Regulation of CHK2 by DNA-dependent protein kinase. *J. Biol. Chem.* **280**, 12041–12050 (2005).
3. M. G. Kemp, L. A. Lindsey-Boltz, A. Sancar, The DNA damage response kinases DNA-dependent protein kinase (DNA-PK) and ataxia telangiectasia mutated (ATM) Are stimulated by bulky adduct-containing DNA. *J. Biol. Chem.* **286**, 19237–19246 (2011).
4. A. S. Doré, A. C. Drake, S. C. Brewerton, T. L. Blundell, Identification of DNA-PK in the arthropods. Evidence for the ancient ancestry of vertebrate non-homologous end-joining. *DNA Repair (Amst.)* **3**, 33–41 (2004).
5. J. Y. Ahn, J. K. Schwarz, H. Piwnica-Worms, C. E. Canman, Threonine 68 phosphorylation by ataxia telangiectasia mutated is required for efficient activation of Chk2 in response to ionizing radiation. *Cancer Res.* **60**, 5934–5936 (2000).
6. Z. Cai, N. H. Chehab, N. P. Pavletich, Structure and activation mechanism of the CHK2 DNA damage checkpoint kinase. *Mol. Cell* **35**, 818–829 (2009).
7. J. Y. Ahn, X. Li, H. L. Davis, C. E. Canman, Phosphorylation of threonine 68 promotes oligomerization and autophosphorylation of the Chk2 protein kinase via the forkhead-associated domain. *J. Biol. Chem.* **277**, 19389–19395 (2002).
8. X. Guo *et al*., Interdependent phosphorylation within the kinase domain T-loop regulates CHK2 activity. *J. Biol. Chem.* **285**, 33348–33357 (2010).
9. A. M. Pregueiro, Q. Liu, C. L. Baker, J. C. Dunlap, J. J. Loros, The Neurospora checkpoint kinase 2: A regulatory link between the circadian and cell cycles. *Science* **313**, 644–649 (2006).
10. M. Wakabayashi, C. Ishii, H. Inoue, S. Tanaka, Genetic analysis of CHK1 and CHK2 homologues revealed a unique cross talk between ATM and ATR pathways in Neurospora crassa. *DNA Repair (Amst.)* **7**, 1951–1961 (2008).
11. J. J. Gamsby, J. J. Loros, J. C. Dunlap, A phylogenetically conserved DNA damage response resets the circadian clock. *J. Biol. Rhythms* **24**, 193–202 (2009).
12. M. Oklejewicz *et al*., Phase resetting of the mammalian circadian clock by DNA damage. *Curr. Biol.* **18**, 286–291 (2008).
13. C. Querfurth *et al*., Circadian conformational change of the Neurospora clock protein FREQUENCY triggered by clustered hyperphosphorylation of a basic domain. *Mol. Cell* **43**, 713–722 (2011).
14. H. Nakashima, J. Perlman, J. F. Feldman, Cycloheximide-induced phase shifting of circadian clock of Neurospora. *Am. J. Physiol.* **241**, R31–R35 (1981).
15. J. C. Dunlap, J. F. Feldman, On the role of protein synthesis in the circadian clock of Neurospora crassa. *Proc. Natl. Acad. Sci. U.S.A.* **85**, 1096–1100 (1988).
16. R. Loewith, M. N. Hall, Target of rapamycin (TOR) in nutrient signaling and growth control. *Genetics* **189**, 1177–1201 (2011).
17. M. Görl *et al*., A PEST-like element in FREQUENCY determines the length of the circadian period in Neurospora crassa. *EMBO J.* **20**, 7074–7084 (2001).
18. Q. He *et al*., CKI and CKII mediate the FREQUENCY-dependent phosphorylation of the WHITE COLLAR complex to close the Neurospora circadian negative feedback loop. *Genes Dev.* **20**, 2552–2565 (2006).
19. A. Sharma, K. Singh, A. Almasan, Histone H2AX phosphorylation: A marker for DNA damage. *Methods Mol. Biol.* **920**, 613–626 (2012).
20. M. Wakabayashi, C. Ishii, S. Hatakeyama, H. Inoue, S. Tanaka, ATM and ATR homologes of Neurospora crassa are essential for normal cell growth and maintenance of chromosome integrity. *Fungal Genet. Biol.* **47**, 809–817 (2010).
21. C. Lundin *et al*., Methyl methanesulfonate (MMS) produces heat-labile DNA damage but no detectable in vivo DNA double-strand breaks. *Nucleic Acids Res.* **33**, 3799–3811 (2005).
22. R. Le Bouffant *et al*., Inhibition of translation and modification of translation factors during apoptosis induced by the DNA-damaging agent MMS in sea urchin embryos. *Exp. Cell Res.* **314**, 961–968 (2008).

23. A. Traven, J. Heierhorst, SQ/TQ cluster domains: Concentrated ATM/ATR kinase phosphorylation site regions in DNA-damage-response proteins. *Bioessays* **27**, 397–407 (2005).
24. G. Park *et al*., Global analysis of serine-threonine protein kinase genes in Neurospora crassa. *Eukaryot. Cell* **10**, 1553–1564 (2011).
25. Y. Sancak *et al*., The Rag GTPases bind raptor and mediate amino acid signaling to mTORC1. *Science* **320**, 1496–1501 (2008).
26. A. Beugnet, A. R. Tee, P. M. Taylor, C. G. Proud, Regulation of targets of mTOR (mammalian target of rapamycin) signalling by intracellular amino acid availability. *Biochem. J.* **372**, 555–566 (2003).
27. S. R. Kimball, A. N. Do, L. Kutzler, D. R. Cavener, L. S. Jefferson, Rapid turnover of the mTOR complex 1 (mTORC1) repressor REDD1 and activation of mTORC1 signaling following inhibition of protein synthesis. *J. Biol. Chem.* **283**, 3465–3475 (2008).
28. K. Hara *et al*., Amino acid sufficiency and mTOR regulate p70 S6 kinase and eIF-4E BP1 through a common effector mechanism. *J. Biol. Chem.* **273**, 14484–14494 (1998).
29. J. Wengrod *et al*., Phosphorylation of eIF2α triggered by mTORC1 inhibition and PP6C activation is required for autophagy and is aberrant in PP6C-mutated melanoma. *Sci. Signal.* **8**, ra27 (2015).
30. V. A. Cherkasova, A. G. Hinnebusch, Translational control by TOR and TAP42 through dephosphorylation of eIF2alpha kinase GCN2. *Genes Dev.* **17**, 859–872 (2003).
31. Q. Liu *et al*., Discovery of 9-(6-aminopyridin-3-yl)-1-(3-(trifluoromethyl)phenyl)benzo[h]-[1,6]naphthyridin-2(1H)-one (Torin2) as a potent, selective, and orally available mammalian target of rapamycin (mTOR) inhibitor for treatment of cancer. *J. Med. Chem.* **54**, 1473–1480 (2011).
32. Q. Liu *et al*., Characterization of Torin2, an ATP-competitive inhibitor of mTOR, ATM, and ATR. *Cancer Res.* **73**, 2574–2586 (2013).
33. L. Lauinger *et al*., Thiolutin is a zinc chelator that inhibits the Rpn11 and other JAMM metalloproteases. *Nat. Chem. Biol.* **13**, 709–714 (2017).
34. C. H. Johnson, H. Nakashima, Cycloheximide inhibits light-induced phase shifting of the circadian clock in Neurospora. *J. Biol. Rhythms* **5**, 159–167 (1990).
35. F. Cesbron, M. Brunner, A. C. Diernfellner, Light-dependent and circadian transcription dynamics in vivo recorded with a destabilized luciferase reporter in Neurospora. *PLoS One* **8**, e83660 (2013).
36. L. Ratnayake, K. K. Adhvaryu, E. Kafes, K. Motavaze, P. Lakin-Thomas, A component of the TOR (Target of Rapamycin) nutrient-sensing pathway plays a role in circadian rhythmicity in Neurospora crassa. *PLoS Genet.* **14**, e1007457 (2018).
37. G. Park *et al*., High-throughput production of gene replacement mutants in Neurospora crassa. *Methods Mol. Biol.* **722**, 179–189 (2011).
38. W. J. Belden *et al*., The band mutation in Neurospora crassa is a dominant allele of ras-1 implicating RAS signaling in circadian output. *Genes Dev.* **21**, 1494–1505 (2007).
39. R. H. D. Davis, F. J., de Serres, Genetic and microbial research techniques for Neurospora crassa. *Methods Enzymol.* **17A**, 79–143 (1970).
40. T. Schafmeier *et al*., Transcriptional feedback of Neurospora circadian clock gene by phosphorylation-dependent inactivation of its transcription factor. *Cell* **122**, 235–246 (2005).
41. L. Lauinger, A. Diernfellner, S. Falk, M. Brunner, The RNA helicase FRH is an ATP-dependent regulator of CK1a in the circadian clock of Neurospora crassa. *Nat. Commun.* **5**, 3598 (2014).
42. T. Schäfer *et al*., Hrr25-dependent phosphorylation state regulates organization of the pre-40S subunit. *Nature* **441**, 651–655 (2006).